Bundle-Shaped Cyclodextrin–Tb Nano-Supramolecular Assembly Mediated by C_{60}: Intramolecular Energy Transfer

Yu Liu,* Guo-Song Chen, Yong Chen, Ning Zhang, Jing Chen, and Yan-Li Zhao

Department of Chemistry, State Key Laboratory of Elemento-Organic Chemistry, Nankai University, Tianjin 300071, P. R. China

ABSTRACT

A bundle-shaped nano-supramolecular assembly possessing numerous luminescent cyclodextrin–Tb polyads and photosensitizing C_{60} units has been constructed through the end-to-end inclusion complexation of cyclodextrin cavities with C_{60}s, and its properties have been comprehensively characterized. Further investigations on the luminescence properties of the cyclodextrin–Tb polyad and the bundle-shaped assembly demonstrate that a pyridine → Tb → C_{60} intramolecualr energy transfer process is operative when a solution of the assembly is exposed to UV light.

Luminescent properties of lanthanide complexes, especially europium and terbium complexes, have been widely exploited, particularly in the fields of bioassay,[1,2] microscopy,[3] and chemical sensors.[4] Functional lanthanide complexes with optimized structural[5] and electronic properties[6−8] represent the recent interests, giving many fascinating utilities in biosystems.[9−11] On the other hand, fullerenes are known to have excellent photosensitizing activities,[12,13] especially under visible and near-infrared lights, which enables them to attract many scientific and technological attentions in material sciences and medicinal chemistry.[14] Recently, benefiting from the good inclusion complexation ability of cyclodextrins (CDs) with various substrate molecules,[15] the construction of functional nano-supramolecular materials or devices using CDs as building blocks has become one of the most interesting research fields.[16,17] For example, Harada et al.[18] constructed a new family of CD assemblies through the inclusion complexation of CDs with adamantane derivatives. Stoddart and co-workers[19] prepared several polyrotaxanes and reviewed a number of CD-mediated aggregates exhibiting significant chemical and biological functions. Tian et al.[20] reported some CD-based new [2]rotaxanes as light-driven molecular shuttles, on which the CD units can shuttle back and forth by alternating the irradiation frequency. We recently constructed a family of nano-supramolecular fullerene assemblies mediated by monomodified or metallobridged β-CDs, which showed good DNA-cleavage abilities under visible light irradiation.[21,22] These approaches provide a new

pathway to prepare functional polymeric CD−fullerene conjugates. In this paper, we report the construction of a well-preorganized nano-supramolecular architecture possessing numerous luminescent CD−Tb polyads and photosensitizing C_{60} units through the end-to-end inclusion complexation of two CD cavities with a C_{60}. This architecture has been comprehensively characterized by ^{1}H NMR, FT-IR, UV−vis, luminescence, powder X-ray diffraction (XRD), thermogravimetric and differential thermal analysis (TG-DTA), scanning electron microscopy (SEM), scanning tunneling microscopy (STM), and transmission electron microscopy (TEM). Further investigations demonstrate that a pyridine → Tb → C_{60} intramolecualr energy transfer process is operative when a solution of this assembly is exposed to UV light.

The CD−Tb polyad **2** was prepared in situ from a reaction of $Tb(NO_3)_3 \cdot 4.5H_2O$ with pyridine-2,6-dicarboxamide-bridged bis(β-CD) **1** (Scheme 1). Elemental analysis data verified the 3:1 **1**:Tb^{3+} coordination stoichiometry in the solid state. Furthermore, the Job's experiment using luminescence spectroscopy was also performed to explore the coordination stoichiometry between **1** and Tb^{3+} in aqueous solution. The Job's plot of **1**/Tb^{3+} system (see Figure S1 in Supporting Informtion) shows a maximum at a molar fraction of 0.25, corresponding to a 3:1 **1**/Tb^{3+} coordination. That means, each Tb^{3+} chelates to three pyridine-2,6-dicarboxamide bridges as tridentate (ONO) ligand: six O atoms and three N atoms complete the nine-coordinated environment of Tb^{3+}, similar to the cases reported by Cheng et al.[23] A further reaction of

* yuliu@nankai.edu.cn.

Scheme 1
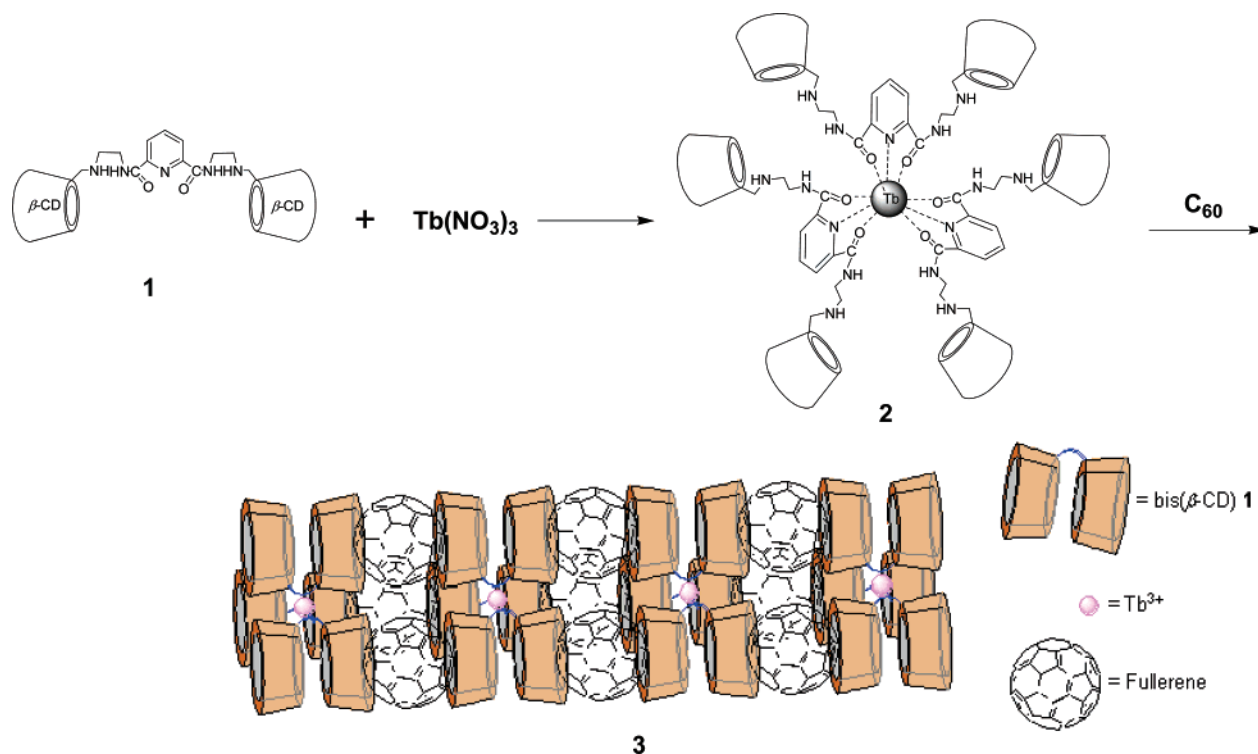
2 with C$_{60}$ produced the assembly **3** in 25% yield (Scheme 1). The FT-IR spectrum of **3** shows a characteristic vibration band at 527 cm^{-1} assigned to C$_{60}$. Moreover, TG-DTA results show that **3** loses 59% of its weight below 700 °C, which demonstrates a 1:3 molar ratio between **2** and C$_{60}$ units, as C$_{60}$ only decomposes over 850 °C.[24] This 1:3 ratio was also verified by the elemental analysis results. Moreover, the NMR signals assigned to the CD's H-3 protons in **2** shift to downfield by 0.1 ppm after reacting **2** with C$_{60}$ (Figure S2). Because H-3 protons are located at the interior of CD cavity and near the wide side, the chemical shift suggests that C$_{60}$ may penetrate into the CD cavity from the wide side.

Additional evidence comes from a comparable study on the UV−vis spectra of bis(β-CD) **1**, polyad **2**, and assembly **3** (Figure S3). The UV−vis spectrum of **1** displays a peak at 270 nm (ϵ = 4270 dm^3 mol^{-1} cm^{-1}) as well as two shoulders at 266 nm (ϵ = 3930 dm^3 mol^{-1} cm^{-1}) and 277 nm (ϵ = 3600 dm^3 mol^{-1} cm^{-1}), which are assigned to the characteristic absorptions of pyridine-2,6-dicarboxamide group. After **1** coordinated with Tb^{3+}, the ϵ values of these maximums increase significantly to 11 330 dm^3 mol^{-1} cm^{-1} (270 nm), 9330 dm^3 mol^{-1} cm^{-1} (265 nm), and 10 330 dm^3 mol^{-1} cm^{-1} (278 nm), respectively, along with the appearance of a ligand-to-metal charge transfer (LMCT) band at 358 nm (ϵ = 1130 dm^3 mol^{-1} cm^{-1}). In the UV−vis spectrum of **3**, these characteristic absorptions show obvious hypsochromic shifts (14−16 nm), accompanied by the peak broadening beyond 350 nm. Moreover, a new peak at 277 nm assigned to the characteristic absorption of C$_{60}$ is also observed in the UV−vis spectrum of **3**. In addition, the toluene extract of assembly **3** gives a UV−vis spectrum that presents the typical bands of C$_{60}$, indicating the partial solubilization of C$_{60}$ by polyad **2** in aqueous solution

arising from the inclusion complexation of β-CDs with C$_{60}$ (Figure S4).

More direct evidence for the formation of **3** come from the microscopic and X-ray diffraction studies. SEM images show that the polyad **2** and the assembly **3** possess obviously different surface morphologies (Figure S5). That is, although both **2** and **3** mainly show the 3D regular structures, the surface size of **3** is much smaller than that of **2**. These results indicate that the introduction of C$_{60}$ changes the macrostructure of **2**. Powder X-ray diffraction (XRD) is a generally used method to characterize CD-based complexes and aggregates, because XRD patterns of the resulting complexes and aggregates should be different from those of native CDs.[25,26] As illustrated in Figure 1, the XRD pattern of polyad **2** strongly resembles that of the free bis(β-CD) **1**, displaying three broad bands below 25°. These phenomena indicate that both **1** and **2** are somewhat amorphous. In
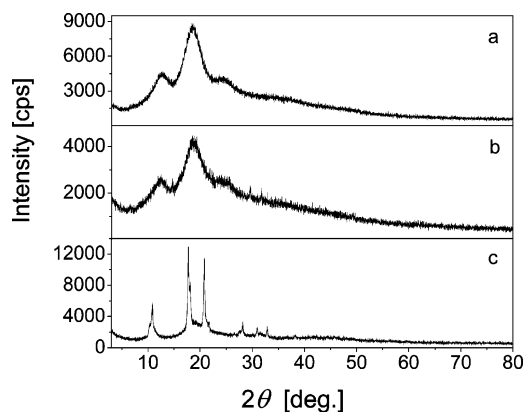

Figure 1. XRD patterns of (a) bis(β-CD) **1**, (b) polyad **2**, and (c) assembly **3**.
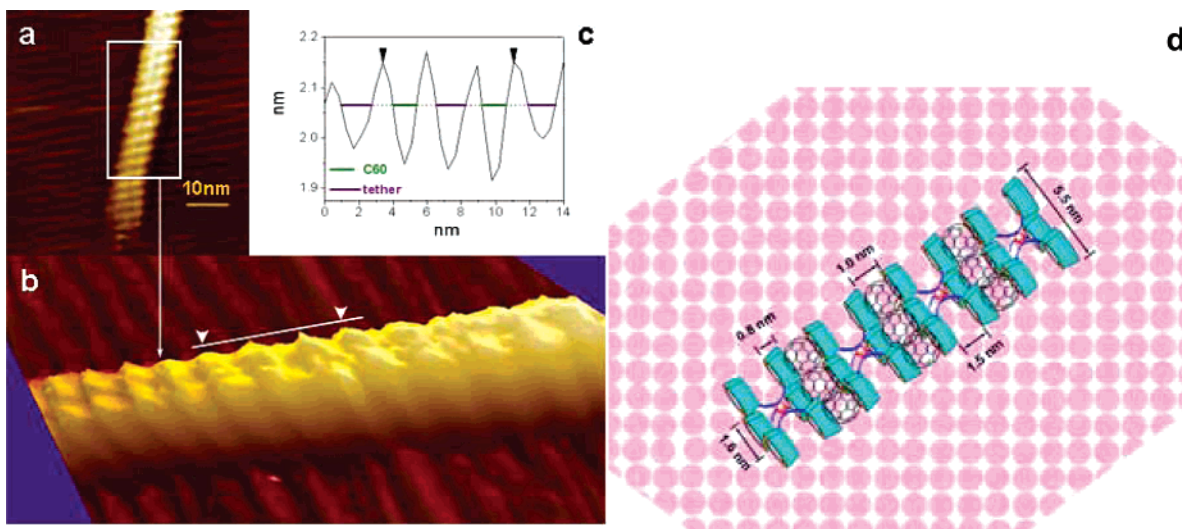
Figure 2. (a,b) STM images of assembly **3** on a HOPG surface (tunneling current 1.0 nA). (c) Line profile of image shown in (b). (d) Schematic structure of **3**.

contrast, the XRD pattern of **3** is unambiguously different from those of **1** and **2,** but resembles that of C_{60}, exhibiting several sharp reflections at $2\theta = 10.8°$ ($d = 8.2$ Å), 17.7° ($d = 5.0$ Å), 20.8° ($d = 4.3$ Å), 28.2° ($d = 3.2$ Å), 30.9° ($d = 2.9$ Å), and 32.9° ($d = 2.7$ Å), which are assigned to the (111), (220), (311), (420), (422), and (333) planes of C_{60},[27] respectively. These results indicate that the introduction of C_{60} not only reorients the polyad **2** upon construction, but also enables an ordered structure of the resulting assembly.

STM images display a fine structure of **3**. Herein, a highly dilute solution of **3** (1×10^{-5} M) was used in the preparation of samples for STM experiments to avoid the aggregation of individual assemblies to fibers. As seen in Figure 2a, the STM image shows a double-lined array with the width of ca. 5.5 nm and the height of ca. 2.2 nm that corresponds to the individual **3**. By analyzing the size and shape of the patterns in Figure 2a, we can deduce that each elliptical bright dot (width ca. 0.9 nm, length ca. 1.8 nm) corresponds to a CD cavity (height 0.8 nm, outer diameter 1.6 nm). Interestingly, as seen in Figure 2c, each bright dot (represented by a peak in Figure 2c) is isolated from the adjacent bright dots by two intervals in different lengths, that is, a short interval (ca. 1.0 nm) assigned to a C_{60} unit and a long interval (ca. 1.5 nm) assigned to a pyridine-2,6-dicarboxamide bridge (1.6 nm calculated by MM2). It is also noteworthy that not only is the height of the assembly chain (ca. 2.2 nm) obviously higher than the diameter of CD cavity (1.6 nm), the height of the wave troughs (ca. 1.9−2.0 nm) is also nearly twice as high as the C_{60} diameter (1.0 nm). This means that the assembly **3** may exist as a double-layered structure on the HOPG surface. That is, the second layer is located under the double-lined array observed in STM images. By combining these results, along with a CPK molecular model study based on the reported C_3 symmetry of pyridine-2,6-dicarboxylic acid/Ln complex,[23] we deduce a possible trefoil bundle-shaped structure of **3**, as illustrated in Figure 2d. Furthermore, after the extraction of the water solution of **3** with toluene, this double-lined array cannot be observed in either the toluene phase or the water phase, indicating the disruption of assembly by withdrawing the C_{60} linker.

TEM imaging gives a further insight into the size and shape of **3**. From TEM images at a higher concentration (1×10^{-4} M), we can find a number of linear structures with a width of 5 nm, which is basically consistent with the STM results. Among them, the longest chain can reach 380 nm (Figure 3a,b), which is joined together through approximately 100 units of the inclusion complex of polyad **2** with C_{60} molecule. Interestingly, the assembly **3** shows the different structural profiles at different concentrations. At a relatively high concentration (1×10^{-4} M), two units of **3** in the similar length (each arrow points one unit of **3**) are located side by side to form an ordered straight array (Figure 3a,b). However, when the solution of **3** was diluted to a lower concentration (5×10^{-6} M), we observed that the original straight double-lined array of **3** changes to the curving single-lined array with a wide length distribution (60−150 nm), which is joined together through approximately 16−40 units of the inclusion complex of polyad **2** with C_{60} molecule (Figure 3c).

Benefiting from the fascinating luminescence property of Tb, the polyad **2** displays a satisfactory luminescence emission in aqueous solution (Figure 4). When excited at 275 nm, a dilute solution of **2** (1×10^{-6} M) exhibited a satisfactory luminescence emission (quantum yield 0.058), giving four characteristic peaks assigned to the $^5D_4 \rightarrow {}^7F_J$ ($J = 3, 4, 5, 6$) transitions of Tb[28] with a intensity ratio of $I(^5D_4 \rightarrow {}^7F_6):I(^5D_4 \rightarrow {}^7F_5):I(^5D_4 \rightarrow {}^7F_4):I(^5D_4 \rightarrow {}^7F_3) = 30.5:62.5:6.5:0.5$. However, in the luminescence spectrum of **3** (1×10^{-6} M calculated as Tb^{3+}), the quantum yield of these emissions decreases to 0.023, and the intensity ratio of $I(^5D_4 \rightarrow {}^7F_6):I(^5D_4 \rightarrow {}^7F_5):I(^5D_4 \rightarrow {}^7F_4):I(^5D_4 \rightarrow {}^7F_3)$ changes to 26.1:69.6:3.6:0.7. Furthermore, when the solutions of **2** and **3** were adjusted to exhibit identical absorption at the excitation wavelength of 275 nm, a more significant luminescence quenching was observed. These results indicate that the introduction of C_{60} significantly alters the luminescence behavior of **2**. Generally, a photoinduced electron transfer
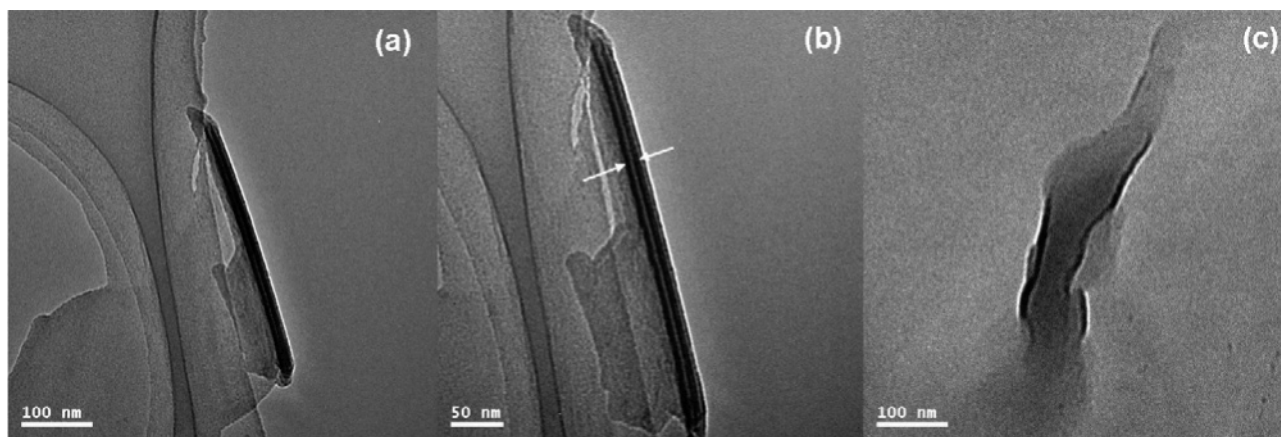
Figure 3. (a) TEM and (b) HR-TEM images of **3** (1×10^{-4} M). (c) TEM images of **3** (5×10^{-6} M).
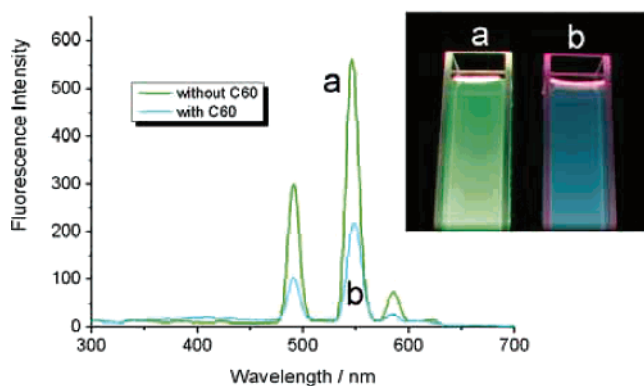

Figure 4. Luminescence spectra of polyad **2** and assembly **3** (1×10^{-6} calculated as Tb^{3+}) in a pH 7.2 Tris-HCl buffer solution; excitation wavelength: 275 nm, slit width 5 nm. (inset) Visible emission observed from (a) polyad **2** and (b) assembly **3**.

(PET) process is often responsible for the luminescence quenching. In the control experiments, the luminescence spectra of polyad **2** in the presence of some benzene derivatives, pyridine derivatives, naphthalene derivatives, and anthracene derivatives, which are widely reported to be able to interact with the fluorophores through a PET process, were obtained and compared with that of free **2**. The results show that the emission of **2** shows no appreciable changes in the presence of benzene and pyridine derivatives but slightly decreases by adding naphthalene and anthracene derivatives. Therefore, we deduce that the PET process is not the main reason for the quenched luminescence of **3**. Another possible reason for the quenched luminescence may be the light absorption by the non-emissive C_{60}, because C_{60} is well-known to have a significant extinction coefficient at the excitation wavelength of 275 nm. Therefore, we compared the luminescence intensity of **2** in the absence and presence of C_{60}. The results show that the change of the luminescence intensity of **2** is negligible after adding a solution of 3 equiv of C_{60} in a minimum amount of toluene/DMF. These results indicate that the luminescence quenching of **2** is attributed to the energy transfer from **2** to C_{60}, but not attributed to the simple extinction effect of C_{60}.

Considering the C_{60} can absorb visible and near-infrared lights, we deduce that an intramolecular energy transfer

process may be mainly responsible for the luminescence quenching. That is, the incoming UV light is absorbed by the pyridine-2,6-dicarboxamide group, and then the coordinated Tb is excited through a ligand-to-metal energy transfer and luminesces. Subsequently, most of the luminescence is absorbed by the C_{60} accommodated in the CD cavities, which leads to the quenched luminescence of **3**.

In this paper, we successfully prepare a luminescent CD−Tb polyad. Subsequently, this polyad is assembled to a trefoil bundle-shaped nano-supramolecular architecture through the inclusion complexation linkage of C_{60}. Under UV-light irradiation, an intramolecular energy transfer process occurs among pyridine, Tb, and C_{60} components in this assembly. Due to these advantages, both the polyad **2** and the assembly **3** may have the potential application in many fields of science and technology involving fullerene.

Supporting Information Available: Synthesis, Job's plot, ^1H NMR spectra, UV−vis spectra, FT-IR spectra, SEM images, and TG-DTA curves of bis(β-CD) **1**, polyad **2**, and assembly **3**, the TGA method to deduce the molecular weight of **3**. This material is available free of charge via the Internet at http://pubs.acs.org.

References

(1) Faulkner, S.; Matthews, J. L. In *Comprehensive Coordination Chemistry II*; Ward, M. D., Ed.; Elsevier: Oxford, United Kingdom, 2004; pp 913−944.
(2) Sammes, P. G.; Yahogliou, G. *Nat. Prod. Rep.* **1996**, 1.
(3) (a) Charbonniere, L.; Ziessel, R.; Guardigli, M.; Roda, A.; Sabbatini, N.; Cesario, M. *J. Am. Chem. Soc.* **2001**, *123*, 2436. (b) Beeby, A.; Clarkson, I. M.; Faulkner, S.; Botchway, S. W.; Parker, A. W.; Parker, D.; Williams, J. A. G. *J. Photochem. Photobiol., B* **2000**, *57*, 83.
(4) Parker, D. *Coord. Chem. Rev.* **1997**, *205*, 109.
(5) Michels, J. J.; Huskens, J.; Reinhoudt, D. N. *J. Am. Chem. Soc.* **2002**, *124*, 2056.
(6) Pope, S. J. A.; Coe, B. J.; Faulkner, S.; Bichenkova, E. V.; Yu, X.; Douglas, K. T. *J. Am. Chem. Soc.* **2004**, *126*, 9490.
(7) Faulkner, S.; Pope, S. J. *J. Am. Chem. Soc.* **2003**, *125*, 10526.

(8) Petoud, S.; Cohen, S. M.; Bünzli, J.-C. G.; Raymond, K. N. *J. Am. Chem. Soc.* **2003**, *125*, 13324.

(9) Hanaoka, K.; Kikuchi, K.; Kojima, H.; Urano, Y.; Nagano, T. *J. Am. Chem. Soc.* **2004**, *126*, 12470.

(10) Corneillie, T. M.; Hetstone, P. A.; Fisher, A. J.; Meares, C. F. *J. Am. Chem. Soc.* **2003**, *125*, 3436.

(11) Glover, P. B.; Ashton, P. R.; Childs, L. J.; Rodger, A.; Kercher, M.; Williams, R. M.; De Cola, L.; Pikramenou, Z. *J. Am. Chem. Soc.* **2003**, *125*, 9918.

(12) (a) Arbogast, J. W.; Darmanyan, A. P.; Foote, C. S.; Diedrich, F. N.; Whetten, R. L.; Rubin, Y.; Alvarez, M. M.; Anz, S. J. *J. Phys. Chem.* **1991**, *95*, 11. (b) Arbogast, J. W.; Foote, C. S. *J. Am. Chem. Soc.* **1991**, *113*, 8886.

(13) Nagano, T.; Arakane, K.; Ryu, A.; Masunaga, T.; Shinmoto, K.; Mashiko, S.; Hirobe, M. *Chem. Pharm. Bull.* **1994**, *42*, 2291.

(14) (a) Guldi, D. M.; Prato, M. *Acc. Chem. Res.* **2000**, *33*, 695. (b) Echegoyen, L.; Echegoyen, L. E. *Acc. Chem. Res.* **1998**, *31*, 593. (c) Prato, M. *J. Mater. Chem.* **1997**, *7*, 1097. (d) Foote, C. S. *Top. Curr. Chem.* **1993**, *169*, 347. (e) Jensen, A. W.; Wilson, S. R.; Schuster, D. I. *Bioorg. Med. Chem.* **1994**, *4*, 767. (f) Da Ros, T.; Prato, M. *Chem. Commun.* **1999**, 663.

(15) Easton, C. J.; Lincoln, S. F. *Modified Cyclodextrins, Scaffolds and Templates for Supramolecular Chemistry*; Imperial College Press: London, 1999.

(16) van den Boogaard, M.; Bonnet, G.; van't Hof, P.; Wang, Y.; Brochon, C.; van Hutten, P.; Lapp, A.; Hadziioannou, G. *Chem. Mater.* **2004**, *16*, 4383.

(17) (a) Liu, Y.; Li, L.; Fan, Z.; Zhang, H.-Y.; Wu, X. *Nano Lett.* **2002**, *2*, 257. (b) Liu, Y.; You, C.-C,; Zhang, H.-Y.; Kang, S.-Z.; Zhu, C.-F.; Wang, C. *Nano Lett.* **2001**, *1*, 613.

(18) (a) Miyauchi, M.; Hoshino, T.; Yamaguchi, H.; Kamitori, S.; Harada, A. *J. Am. Chem. Soc.* **2005**, *127*, 2034. (b) Miyauchi, M.; Harada, A. *J. Am. Chem. Soc.* **2004**, *126*, 11418.

(19) (a) Badjić, J. D.; Nelson, A.; Cantrill, S. J.; Turnbull, W. B.; Stoddart, J. F. *Acc. Chem. Res.* **2005**, *38*, 723. (b) Tseng, H. R.; Vignon, S. A.; Stoddart, J. F. *Angew. Chem., Int. Ed.* **2003**, *42*, 1491. (c) Horn, M.; Ihringer, J.; Glink, P. T.; Stoddart, J. F. *Chem.—Eur. J.* **2003**, *9*, 4046.

(20) (a) Qu, D.-H.; Wang, Q.-C.; Tian, H. *Angew. Chem., Int. Ed.* **2005**, *44*, 5296. (b) Wang, Q. C.; Qu, D. H.; Ren, J.; Chen, K. C.; Tian, H. *Angew. Chem., Int. Ed.* **2004**, *43*, 2661.

(21) Liu, Y.; Wang, H.; Liang, P.; Zhang, H.-Y. *Angew. Chem., Int. Ed.* **2004**, *43*, 2690.

(22) Liu, Y.; Wang, H.; Chen, Y.; Ke, C.-F.; Liu, M. *J. Am. Chem. Soc.* **2005**, *127*, 657.

(23) Zhao, B.; Chen, X.-Y.; Cheng, P.; Liao, D.-Z.; Yan, S.-P.; Jiang, Z.-H. *J. Am. Chem. Soc.* **2004**, *126*, 15394.

(24) Chen, D.; Sarid, D. *Phys. Rev. B* **1994**, *49*, 7612.

(25) Yang, Y.-W.; Chen, Y.; Liu, Y. *Inorg. Chem.* **2006**, *45*, 3014.

(26) (a) Okumura, H.; Kawaguchi, Y.; Harada, A. *Macromolecules* **2001**, *34*, 6338. (b) Harada, A.; Suzuki, S.; Okada, M.; Kamachi, M. *Macromolecules* **1996**, *29*, 5611.

(27) (a) Li, F.; Mao, Z.; Jia, Y.; Chen, Z.; Zhang, S.; Zhou, G.; Wang, D. *Rengong Jingti Xuebao* **1996**, *25*, 164 (in Chinese). (b) Field, C. N.; Hamley, P. A.; Webster, J. M.; Gregory, D. H.; Titman, J. J.; Poliakoff, M. *J. Am. Chem. Soc.* **2000**, *122*, 2480.

(28) (a) Amaud, N.; Vaquer, E.; Georges, J. *Analyst* **1998**, *123*, 261. (b) Reineke, T. M.; Eddaoudi, M.; Fehr, M.; Kelley, D.; Yaghi, O. M. *J. Am. Chem. Soc.* **1999**, *121*, 1651.

NL061393O